CONF-811141--1

CORROSION-INDUCED CHANGES IN PORE-SIZE DISTRIBUTIONS OF FUEL-MATRIX MATERIAL*

P. Krautwasser† and W. P. Eatherly

Metals and Ceramics Division
Oak Ridge National Laboratory
P. O. Box X
Oak Ridge, Tennessee USA 37830

For Presentation at the Colloquium on the Transport of Fission Products in Matrix and Graphite

Berlin, FRG

November 9–11, 1981

---

*Research sponsored by the Office of Nuclear Power Systems, U. S. Department of Energy, under contract W-7405-eng-26 with Union Carbide Corporation and by the German Government and the State of Nordrhein-Westfalen through the Project "HBK."

†On assignment from KFA Juelich.

CORROSION-INDUCED CHANGES IN PORE SIZE DISTRIBUTIONS OF FUEL MATRIX MATERIAL*

P. Krautwasser† and W. P. Eatherly
Oak Ridge National Laboratory

Introduction

In order to understand the mechanism of metallic fission-product adsorption and desorption as well as diffusion in graphitic materials, a detailed knowledge of the material microstructure is essential. Different types of graphitic matrix material used or to be used in fuel elements of the German HTR Program were measured at ORNL in cooperation with the Hahn-Meitner-Institut Berlin. Actual measurements of fission product diffusion and adsorption/desorption were performed at HMI Berlin.

Material

The materials studied were:

A3-3 (1800°C), a material consisting of natural graphite and electrographite with a binder of phenolformaldehyde resin. The final heat treatment of the material was at 1800°C.

A3-3 (1800°C) with different degrees of CO_2 oxidation (corrosion), ranging from 0 to 5% weight loss.

A3-3 (1950°C), an A3-3 material with a final heat treatment at 1950°C to increase strength and decrease reactivity.

A3-27 (1950°C), an alternate material to A3-3 consisting of natural graphite, electrographite, and a binder based on in-place polymerization of phenol and hexamethylene tetramine. The final heat treatment was 1950°C.

Methods

Geometric densities at low Hg pressure and mercury porosimetry were measured with an Aminco Porosimeter modified with precision pressure gauges and to permit subatmospheric pressure measurements. Apparent densities in helium and inner surface areas were obtained with a classical BET apparatus designed and built at ORNL. The micropore size-distributions were derived from Small Angle X-Ray Scattering (SAXS) curves determined with the 10-meter SAXS facility at ORNL. Lattice parameters were measured by standard Debye-Scherrer techniques on powder as well as on solid samples.

---

*Research sponsored by the Office of Nuclear Power Systems, U. S. Department of Energy under contract W-7405-eng-26 with Union Carbide Corporation and by the German Government and the State of Nordrhein-Westfalen through the Project "HBK."

†On assignment from KFA Juelich.

Results

Oxidation of A3–3 (1800°C) Matrix Material. An increase in weight loss during oxidation of the material leads to an increase of pores in the diameter size range of 1.5 to 20 nm (SAXS) and of 0.4 to 1.5 μm (Hg porosimetry) as shown in Table 1 and Fig. 1. This is accompanied with an increase in accessible pore volume as determined by the apparent material density in helium as well as a pronounced increase in total BET surface area. Conversely, as might be expected, the inaccessible pore volume decreases.

The sample with the smallest weight loss (0.1 wt %) shows a decrease in concentration of the very small pores with D = 1.0 μm. This indicates that at the beginning of oxidation the existing fine pores are enlarged. Further oxidation leads, in addition, to the development of micropores smaller than 2.0 μm.

Some data of the samples with 3 and 5% weight loss are inconsistent with the other results. A recalculation of the initial densities from the densities of the oxidized samples and the given weight loss yield a low initial density for the 3% sample and a high value for the sample with 5% weight loss. The differences in other material properties may therefore be in part or entirely due to differences in the initial sample microstructure.

A3–3 Material Heat Treated at 1950°C. Compared to the A3–3 material heat treated at 1800°C, the increase in heat-treatment temperature to 1950°C leads to a decrease of pores in the diameter range of 10 to 20 nm (SAXS) and in the range of 1.0 to 2.5 μm, as shown in Table 2. In this wide range, the peak of the pore size distribution shifts with increasing temperature from D = 1.8 μm to D = 0.9 μm (Fig. 2). This shift as well as the decrease in larger pores lead to a lower BET surface area, accessible pore volume, and apparent density in helium. An increase in inaccessible pore volume is caused by a shift of the pore size distribution to smaller pores and therefore an increase in small micropores with $D \leq 5$ nm, as seen by SAXS. The observed reduction of c-lattice spacing with heat treatment, especially in the binder, leads to an increase in bulk density.

A3–27 Material Heat Treated at 1950°C. Comparing A3–27 (1950°C) with A3–3 (1950°C), the difference in binder polymerization leads to a higher bulk density, a somewhat lower accessible pore volume, and a decrease in pores with D > 0.4 μm (Table 2). The maximum in pore size distributions of A3–27 material is at D = 1.25 μm, in between the peaks of the A3–3 (1800°C) and A3–3 (1950°C) materials. The inaccessible pore volume in A3–27 (1950°C) is about the same as in A3–3 (1950°C).

Compared to A3–3 (1800°C), the increase in final heat treatment leads as well as in A3–3 (1950°C) to an increase in pores ranging from 1.0 to 5.0 nm and a decrease in 5.0 to 20.0 nm pores.

Conclusions

The oxidation series of A3–3 (1800°C) samples shows the anticipated effects of an immediate increase in total surface area (BET) and accessible void volume at the very lightest burn-offs. This is consistent with graphite behavior generally under steam or carbon dioxide oxidation but

accentuated here presumably due to the nongraphitizable binder and low heat-treatment temperature. The pore textures coarsen, although the effects are more marked in the micropore region (< 20 nm diameter) than in the macropore region (> 0.4 μm diameter).

Both A3-3 (1950°C) and A3-27 (1950°C) show a normal behavior to increased heat-treatment temperature with increased densification and inaccessible pore volume and decreased total surface area (BET) and accessible pore volume. These effects are attributable to the resin binder shrinkage as the last hydrogen is eliminated and incipient crystallization occurs. The lack of well-developed long-range order leads concurrently to an increase in the micropore volume (< 5 nm diam).

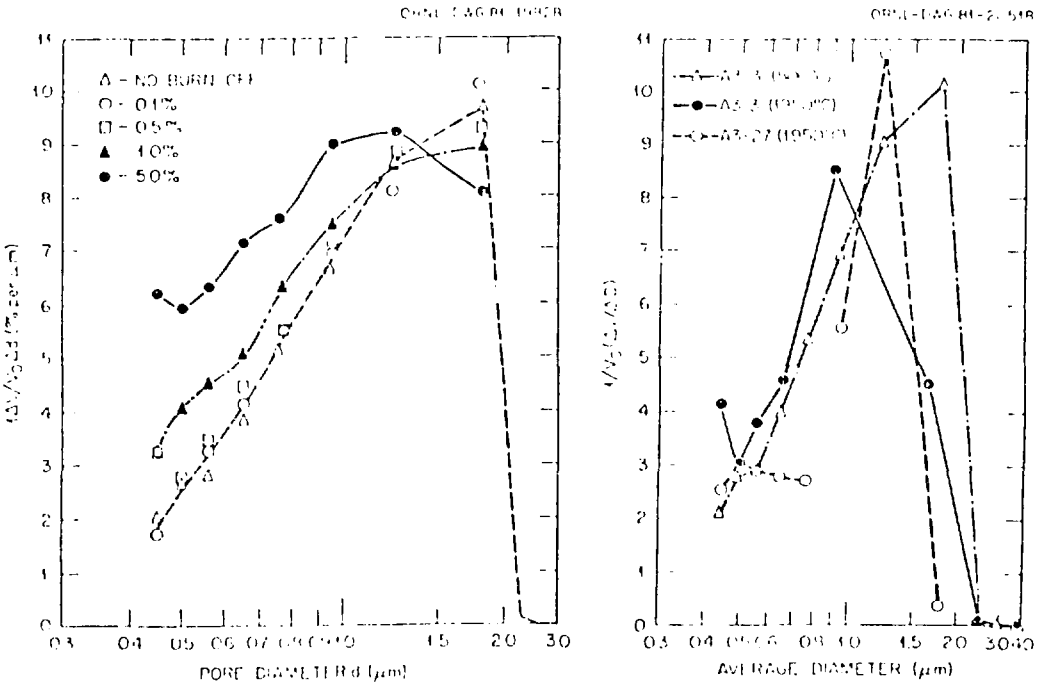

Figs. 1 and 2. Size distribution of pores ranging from 0.4 to 4.0 μm in diameter in oxidized material (left) and in A3-3 (1800°C), A3-3 (1950°C), and A3-27 (1950°C) (right).

Table 1. Data on Oxidized A3-3 (1800°C) Material. Original densities were calculated from oxidized densities and quoted burn-offs. Inaccessible pore volume assumes a theoretical density of 2.27 g/cm^3.

Sample No.	Burn Off (%)	Bulk Densities (g/cm^3)		Pore Volumes (%)				Surface Area (m^2/cc)
		Original	Oxidized	> 1 μm	> 0.4 μm	Accessible	Inaccessible	
1	0	1.700	1.700	11.62	14.79	15.80	9.32	0.236
5	0.1	1.699	1.697	11.15	14.49	16.53	8.72	0.437
7	0.5	1.694	1.686	9.85	13.12	20.21	5.53	1.70
4	1.0	1.697	1.680	10.00	13.68	19.69	6.30	7.19
6	5.0	1.745	1.658	9.58	14.34	22.49	4.48	11.2
8	3.0	1.664	1.614			23.54	5.36	13.3

Table 2. Characterization of Three Fuel Matrix Types. Where applicable, values are given as means with population standard deviations and, in parentheses, number of samples.

Material Type	Bulk Density (g/cm^3)	Pore Volumes (%)				Surface Area (m^2/cc)
		> 1 μm	> 0.4 μm	Accessible	Inaccessible	
A3-3 (1800°)	1.706 ± 0.009 (2)	11.62	14.79	14.56 ± 1.76 (2)	10.28 ± 1.3 (2)	0.224 ± 0.016 (2)
(1950°)	1.724 ± 0.031 (4)	5.39	9.71	11.14 ± 1.38 (4)	12.93 ± 0.74 (4)	0.181 ± 0.006 (2)
A3-27 (1950°)	1.766 ± 0.002 (2)	5.82	7.04	9.58 ± 0.18 (2)	12.65 ± 0.27 (2)	